AD-A043 563 CALIFORNIA INST OF TECH PASADENA F/G 20/4
INTRODUCTION TO THE SCALING OF AQUATIC ANIMAL LOCOMOTION,(U)
JUL 77 T Y WU N00014-76-C-0157
UNCLASSIFIED E-97B-50 NL

| OF |
AD
A043 563

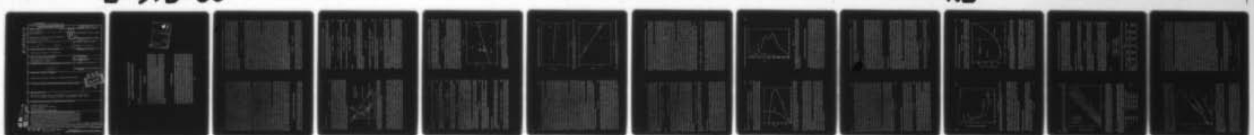

END
DATE
FILMED
9-77
DDC

Unclassified

SECURITY CLASSIFICATION OF THIS PAGE (When Data Entered)

ADA043563

REPORT DOCUMENTATION PAGE

READ INSTRUCTIONS BEFORE COMPLETING FORM

1. REPORT NUMBER (14) E-97B-50	2. GOVT ACCESSION NO. (11)	3. RECIPIENT'S CATALOG NUMBER
4. TITLE (and Subtitle) (6) Introduction to the Scaling of Aquatic Animal Locomotion,		5. TYPE OF REPORT & PERIOD COVERED
		6. PERFORMING ORG. REPORT NUMBER E-97B-50
7. AUTHOR(s) (10) T. Y. Wu Theodore Y./Wu		8. CONTRACT OR GRANT NUMBER(s) (15) N00014-76-C-0157
9. PERFORMING ORGANIZATION NAME AND ADDRESS California Institute of Technology		10. PROGRAM ELEMENT, PROJECT, TASK AREA & WORK UNIT NUMBERS
11. CONTROLLING OFFICE NAME AND ADDRESS Office of Naval Research The Department of the Navy Arlington, VA 22217		12. REPORT DATE (11) July 1977
		13. NUMBER OF PAGES 30
14. MONITORING AGENCY NAME & ADDRESS (if different from Controlling Office) (12) 17p.		15. SECURITY CLASS. (of this report)
		15a. DECLASSIFICATION/DOWNGRADING SCHEDULE

16. DISTRIBUTION STATEMENT (of this Report)

Approved for public release: Distribution unlimited

17. DISTRIBUTION STATEMENT (of the abstract entered in Block 20, if different from Report)

18. SUPPLEMENTARY NOTES

Reprints from the Book: Scale Effects in Animal Locomotion, ed. T. J. Pedley, Academic Press : London/New York 1977.

19. KEY WORDS (Continue on reverse side if necessary and identify by block number)

Fishing swimming
Micro-organism locomotion
Scaling effects
Biomechanics and energetics.

20. ABSTRACT (Continue on reverse side if necessary and identify by block number)

This introductory lecture attempts to discuss the scaling problems related to the locomotion of aquatic animals in two major categories characterized by low and high Reynolds numbers of swimming motion. In the low-Reynolds-number flow regime it first gives a brief survey of flagellar and ciliary locomotion in order to ascertain the different key parameters that play a role. The hydromechanical and physiological performance of a group of micro-organisms, of different sizes but otherwise similar in their organization from the scaling point of view, is examined.

In the high-Reynolds-number category, discussions of the scaling problems include the carangiform and lunate-tail locomotion of different groups of fishes and cetaceans, with consideration of hydromechanical efficiency and physiological function. The discussion is based on the data of both comparative zoology and dynamical similarity.

DD FORM 1 JAN 73 1473 EDITION OF 1 NOV 65 IS OBSOLETE
S/N 0102-014-6601

Unclassified

SECURITY CLASSIFICATION OF THIS PAGE (When Data Entered)

071 550

13. Introduction to the Scaling of Aquatic Animal Locomotion

T. Y. WU
California Institute of Technology, Pasadena, California, U.S.A.

ABSTRACT

This introductory lecture attempts to discuss the scaling problems related to the locomotion of aquatic animals in two major categories characterized by low and high Reynolds numbers of swimming motion. In the low-Reynolds-number flow regime it first gives a brief survey of flagellar and ciliary locomotion in order to ascertain the different key parameters that play a role. The hydromechanical and physiological performance of a group of micro-organisms, of different sizes but otherwise similar in their organization from the scaling point of view, is examined.

In the high-Reynolds-number category, discussions of the scaling problems include the carangiform and lunate-tail locomotion of different groups of fishes and cetaceans, with consideration of hydromechanical efficiency and physiological function. The discussion is based on the data of both comparative zoology and dynamical similarity.

INTRODUCTION

It is most gratifying to see this Cambridge Symposium take on the main theme of *scaling and similitude* in animal locomotion. Its importance for the future development of biological science has become increasingly recognized. A timely exploration of this theme, which is the objective of this meeting, will certainly add strength to and point out new, rewarding directions for current research activities such as those presented at the International Symposium on Swimming and Flying in Nature held in Pasadena in July 1974.

It is a great privilege to have been called upon by Professor Lighthill and Professor Weis-Fogh to give an introductory talk on the influence of size on the different types of aquatic locomotion found in various groups of animals.

In accepting the call I fully realize that the total range of subject-matter to be covered is very extensive and it would be hard to emulate Professor Lighthill's elucidation of the scaling aspects of some 10 groups of aquatic animals at the 1973 Duke University Conference. I feel, nevertheless, that I have benefited from this exciting challenge, for already I have found that important and difficult problems in fluid mechanics have been illuminated by studies in metabolism and chemical energy conversion, and vice versa. For example, we can actually make a better estimate of the drag of a fish from biological measurements than from direct flow measurement, because the latter is formidably hard. This underlines the importance of close collaboration between scientists from different fields engaged in interdisciplinary research on topics such as animal locomotion. In this regard I would like to acknowledge with appreciation the co-operation of the two groups at Cambridge, under Sir James Lighthill and Professor Torkel Weis-Fogh respectively, as well as that of many other colleagues from all over the world.

I would like to discuss the scaling problems of aquatic animal locomotion in two major categories, characterized respectively by low and high Reynolds numbers of the swimming motion, which are broadly equivalent to aquatic animals of microscopic and macroscopic size. In the low-Reynolds-number regime I shall give a brief survey of flagellar and ciliary propulsion in order to ascertain the key parameters underlying the hydromechanical and physiological performance of the two groups of micro-organisms. Here the limited range of animal sizes, swimming speeds, and beat frequencies observed in specific groups, coupled with the very limited data available on their energy conversion processes, show that a lot more information is required before a good understanding can be reached.

In the high-Reynolds-number category, I shall concentrate on the scaling problems of carangiform and lunate-tail locomotion of different groups of fishes and cetaceans, considering their hydromechanical efficiency and physiological functions on the basis of data from both comparative zoology and dynamical similarity. This is an area where experimental results are relatively abundant, and there has recently been considerable research activity, so that a more refined investigation of the scaling problem is possible. Current studies combining both physiology and dynamics promise further progress which may have far-reaching effects, as I hope to point out later.

LOCOMOTION OF MICRO-ORGANISMS

The two major kinds of microscopic organisms to be discussed here are the flagellates and the ciliates. In general they have a maximum linear dimension smaller than 1 mm, with a majority of them being much smaller. Flagellates

propel themselves through an aqueous medium by performing undulatory movements of a long thin flagellum (or several flagella) in the form of a planar, helical, or a general three-dimensional wave. Ciliary propulsion utilizes the co-ordinated effort of a large number of *flagella-like organelles*, called cilia, which are distributed over the cell membrane, and wave in a manner known as 'metachronism'. Both flagellates and ciliates swim in aqueous media, attaining a characteristic velocity, V, in such a way that the Reynolds number

$$\mathrm{Re} = Vl/\nu \tag{1}$$

is very low. Here $\nu = 0{\cdot}01\ \mathrm{cm^2\,s^{-1}}$ is the kinematic viscosity of water, and l is the length of the organism. Typical values of the Reynolds number are around 10^{-3} for spermatozoa, 10^{-6} for most bacteria, and in the range $0{\cdot}01 < \mathrm{Re} < 1$ for various ciliates (the Reynolds number based on ciliary length l_c is considerably smaller). At these low Reynolds numbers, all the inertial effects, both of the liquid and of the organism, become insignificant. Consequently, hydromechanical calculations of flagellar and ciliary propulsion are generally based on neglecting the inertial effects, leaving the viscous stress and pressure as the only quantities that need be considered in the momentum balance for given swimming movements.

From the laws of motion, the net momentum and net angular momentum of the fluid surrounding a self-propelling micro-organism, swimming at constant velocity, must be zero. However, the backward drag force and the equal and opposite thrust acting on a swimming micro-organism cannot be separated, as they can for a large aquatic animal (as we shall see), and must be dealt with together. For a long, thin organelle such as a flagellum or a cilium, the forces tangential and perpendicular to its centerline, denoted by F_s and F_n respectively, which it exerts on the fluid while moving with tangential and normal velocities V_s and V_n, depend mainly on its length l and not on its transverse dimensions. Calculations of these forces can be considerably simplified by means of the "resistive-force theory", which was first developed for flagellar applications by Hancock[33] and Gray and Hancock,[31] was extended to helical movements by Chwang and Wu,[25] and was recently refined further by Lighthill.[48, 49] It provides a simple relationship between the force and the velocity in the form

$$F_s = C_s V_s l, \qquad F_n = C_n V_n l, \tag{2}$$

where C_s and C_n are the resistive force coefficients which depend on the transverse dimensions and wavelength of the body but not on its velocity. Both C_s and C_n are proportional to the (dynamic) viscosity coefficient of the fluid, μ (equal to the kinematic viscosity, ν, times the density $1\ \mathrm{g\,cm^{-3}}$).

The ratio of C_s to C_n, or

$$\gamma = C_s/C_n \tag{3}$$

plays an important role in swimming propulsion since its value (always <1) determines what type of undulatory motion will give the optimum forward velocity or optimum efficiency, as first elucidated by Lighthill (Refs 43, p. 442; 48, p. 122). I shall try to recapitulate his argument by considering the ideal case of *zero-thrust swimming* of a flagellum (such as that of a sperm detached from the cell body, or of a spirochete). I shall deal solely with the translational motion, leaving the possible angular motion and all further details to the literature. (The same argument can be applied, qualitatively at least, to larger elongated animals.)

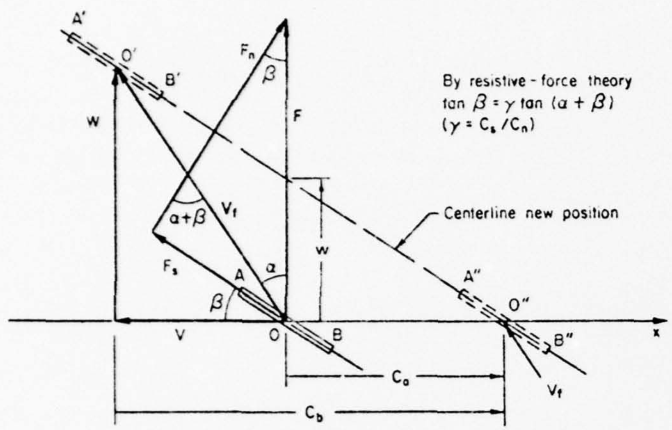

FIG. 1. A resistive-force theory diagram. A segment AB of an elongated body in undulatory motion moves with velocity $\mathbf{V}_f$ and exerts a force $\mathbf{F}$ on the fluid in a zero-thrust propulsion. Its lateral velocity is W *relative to the animal's mean position and* w *relative to the water.* The wave velocity is c_a relative to the water and c_b relative to the body.

Figure 1 shows a segment AB of an elongated animal supposed to be performing a plane or helical wave, and achieving a swimming velocity V in the negative x-direction. In the ideal case of zero thrust (or zero x-component force), the force $\mathbf{F}$ exerted by the segment on the fluid can only be in a transverse direction as shown. Nevertheless there is a forward tangential component F_s along the centerline of the body when the latter is inclined to the path of swimming at an angle β. (Figure 1 may be envisaged as in the plane of a planar wave, or, in the case of a helical wave, in the plane tangential to the helical movement of the segment in question.) The segment, under the combined traction of F_s and the normal component of force, F_n, will move to a new position $A'B'$ with velocity $\mathbf{V}_f$ which has the forward x-component V and a transverse component W. Clearly, we have

$$F_s = F \sin\beta, \qquad F_n = F \cos\beta, \tag{4}$$

and

$$V_s = V_f \sin(\alpha + \beta), \qquad V_n = V_f \cos(\alpha + \beta), \tag{5}$$

where α is the angle between $\mathbf{F}$ and $\mathbf{V}_f$. Substituting (4) and (5) in (2) yields

$$\tan\beta = \gamma \tan(\alpha + \beta). \tag{6}$$

The angle α vanishes when $\beta = 0$ or $\pi/2$, and achieves a maximum when

$$\beta = \beta_m = \arctan \gamma^{1/2}, \tag{7}$$

giving

$$V_{\max}/W = \tan\alpha_{\max} = \tfrac{1}{2}(1 - \gamma)/\gamma^{1/2}. \tag{8}$$

In the meantime the constant phase of the body wave has been propagated backwards to reach position $A''B''$ (which would now be occupied by a new segment of the body) with wave (phase) velocity c_a relative to the water, or with wave velocity

$$c_b = c_a + V \tag{9}$$

in the body frame of reference. Since $W/c_b = \tan\beta$ (see Fig. 1),

$$V_{\max}/c_b = \tan\alpha_m \tan\beta_m = \tfrac{1}{2}(1 - \gamma). \tag{10}$$

The lateral velocity of the segment relative to the water, w, is equal to $W(c_a/c_b)$, which when $\beta = \beta_m$ assumes a value such that

$$\frac{w}{W} = \frac{c_a}{c_b} = \tfrac{1}{2}(1 + \gamma). \tag{11}$$

The above results agree with Lighthill's (Ref. 48, p. 123). An important consequence is that for fixed W (or c_b), $V_{\max}$ decreases with increasing γ, and vanishes at $\gamma = 1$, which means self-propulsion in the present case (of zero thrust) would be impossible when $C_s = C_n$.

A more general situation arises when a flagellum or a ciliary system has a passive cell body to propel so that each segment must on average have its force $\mathbf{F}$ directed both sidewise and somewhat forward. The efficiency may then be defined as the ratio of useful work done by the forward component of $\mathbf{F}$ in propelling the animal forward at speed V, to the power required which is $\mathbf{F}\cdot\mathbf{V}_f$. The values of $V_{\max}$ and V at the maximum efficiency can also be

calculated. Lighthill[48] showed that the value of V at maximum efficiency ($\eta = \eta_{max}$) is

$$V/c_b = 1 - \gamma^{1/2} \quad \text{and} \quad \eta_{max} = (1 - \gamma^{1/2})^2. \tag{12}$$

This value of V is not much less than V_{max} (Eqn 10), even when $\gamma = 0{\cdot}2$.

Detailed analysis has produced the following expressions for the force coefficients in the low Reynolds number case

$$C_s = \frac{2\pi\mu}{\ln(2q/b) - 1/2}, \qquad C_n = \frac{4\pi\mu}{\ln(2q/b) + 1/2}, \tag{13}$$

where b is the cross-sectional radius of the thin segment, and q is a quantity depending on body shape and certain wave parameters. Lighthill[49] contended that for flagellar waves with wavelength λ it is accurate to take

$$q = 0{\cdot}09\lambda, \tag{14}$$

and to delete the term $-1/2$ in the denominator of the expression for C_s. (The values of q for rigid slender bodies of various shapes are given by Batchelor,[8] Tillett,[61] Cox[26]). The value of γ, according to these formulas, lies in a range between 0·6 and 0·7 and is not close to 0·5 as earlier theories have commonly assumed. The corresponding efficiency is therefore about 0·05 for flagellar propulsion, which is rather low, and $V/c_b \simeq 0{\cdot}2$. Lighthill[46] noted that for swimming snakes γ is likely to be about 0·1, leading to $\eta \simeq 0{\cdot}5$ and $V/c_b \simeq 0{\cdot}7$.

Another important feature of flagellar propulsion is that the maximum inclination of a plane flagellar wave, or the pitch angle of a helical flagellar wave, should, for maximum speed, be

$$\beta_{max} \simeq 40^\circ \tag{15}$$

(from Eqn 7) for γ around 0·6. This figure is close to the value for minimum power output, and comparable values are indeed observed.

With this introduction we now proceed to discuss the problems of flagellar and ciliary propulsion separately.

Flagellar Propulsion

The mechanical power needed for a flagellar organism of length l_f to swim at velocity V may be readily estimated by applying the resistive theory, giving

$$P_f = F_s V_s + F_n V_n = C_n(\gamma V_s^2 + V_n^2) l_f \simeq 50 \mu V^2 l_f, \tag{16}$$

where the constant factor 50 is borne out by detailed calculation to be typical of flagellar movement. It is based on the observation that there is not much difference in diameter (about 0·2 μm) between the flagella of different

species (excluding the bacterial flagella), and λ/b is typically between 100 and 200, though the length l_f may vary considerably from one species to another. Additional power is further required to overcome the drag of a passive cell body (of a three-dimensional form with length l_b say), if any, which is

$$P_b = \text{const.} \quad \mu V^2 l_b. \tag{17}$$

The value of P_b is generally smaller than that of P_f.

To proceed with a scaling analysis we need to know the chemical energy input per flagellar beat (say E_c); this can in principle be obtained from the measured rate of dephosphorylation of ATP (the chemical compound adenosine triphosphate) by the flagellum. Such information, however, is extremely scarce. Under the circumstances it has been suggested (see Alexander,[1] p. 40) that for protozoic flagella having the well-known arrangement of 9 + 2 pairs of micro-fibrils running along them, the maximum chemical energy input of a flagellum is likely to be proportional to its length l_f (or,

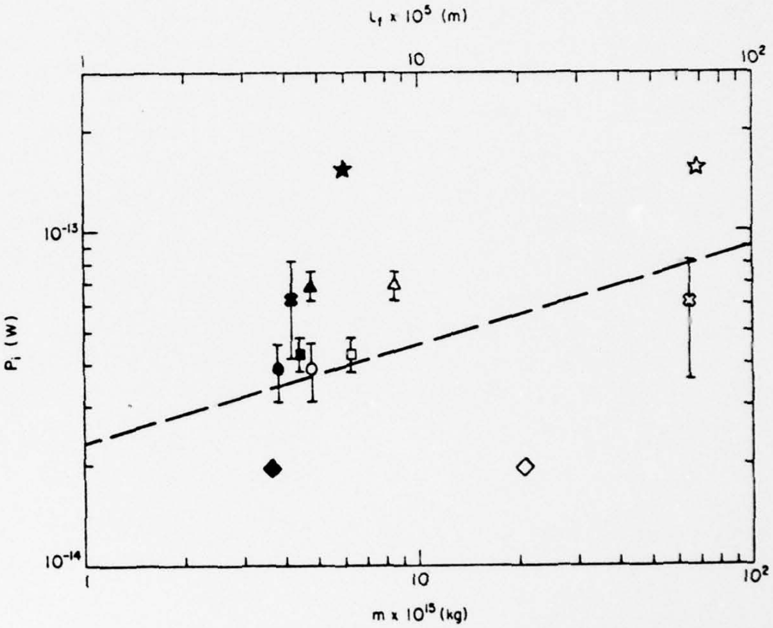

FIG. 2. Variation of chemical power input P_i of flagellates with their flagellar length l_f (in solid symbols) and mass m (in open symbols). × —*Colobocentrotus atrafus*; ○—*Strongylocentrotus purpuratus*; □—*Lytechinus pictus*; △—*Ciona intestinalis*; ◇—*Chaetopterus variopedatus*; ★—Bull sperm. Experimental data from Brokaw and Gibbons.[24] The slope of the dotted regression line is 0·28.

equivalently, to the mass of the flagellum since its cross-sectional diameter is uniform and constant). From this assumption and Eqn (16) is would follow that the swimming velocity V is scale-independent.

The experimental data which have made this preliminary study possible are taken from Brokaw and Gibbons[24] who investigated the process of converting the chemical energy of ATP into the mechanical work of sliding between the doublet tubules of the axoneme, and hence of generating particular flagellar waves, in six different species of spermatozoa. Figure 2 shows the dependence of chemical power input of the flagellates, P_i, on the flagellar length l_f (which is 3 to 15 times the cell-body length) and the total mass m of the organism. Although a regression line can be drawn by the method of least squares for the $\log P_i - \log m$ relation, with slope 0·28, the data are considered to be too scattered for a confident conclusion to be drawn. The short range of flagellar length l_f covered by these species makes determination of the $P_i - l_f$ relation difficult, but, from these results at least, P_i is clearly far from being proportional to l_f as predicted.

The difficulties seem to stem from the apparent lack of correlation between l_f and m, as can be seen from Fig. 2. This is in fact not surprising since the thrust required from each segment of a long flagellum to balance the drag force on the cell body is very small. Thus changes in mass, and hence drag force, will involve only very slight modification of the propulsive mechanism, which will still be approximately described by the zero-thrust theory outlined above. This implies that the flagellar length l_f (or the total cell length l) may not be the pertinent parameter to use in scaling; perhaps future experimental results will help settle this point.

We present in Fig. 3 the variation of swimming velocity V with m, for which a least square fit yields $V = \text{const.}\, m^{-0\cdot 04}$, ie. V is virtually independent of body mass. This is in sharp contrast with the case of large animal locomotion, as we shall see in the discussion of the scaling of fish swimming.

The nondimensional quantity

$$\mathscr{E} = P/mgV, \tag{18}$$

where P stands for either the chemical power input or the mechanical power required, and g is the acceleration of gravity, provides a useful measure of the relative merit of different propulsive systems. If an animal expends power $P = \mathrm{d}E/\mathrm{d}t$ to keep moving along a straight level path at speed $V = \mathrm{d}x/\mathrm{d}t$, where x is distance measured along the path, the ratio $P/mgV = (mg)^{-1}\,\mathrm{d}E/\mathrm{d}x$ therefore gives the energy expenditure to transport unit weight unit distance. The parameter $\mathscr{E}$ may thus be called the "specific energy cost" of transport (cf. the "net cost of transport" as defined by Alexander). It has been used by von Karman and Gabrielli[66] to evaluate the comparative merits of 14 classes of transportation vehicle, and by Schmidt-Nielsen,[57] Tucker,[63, 65]

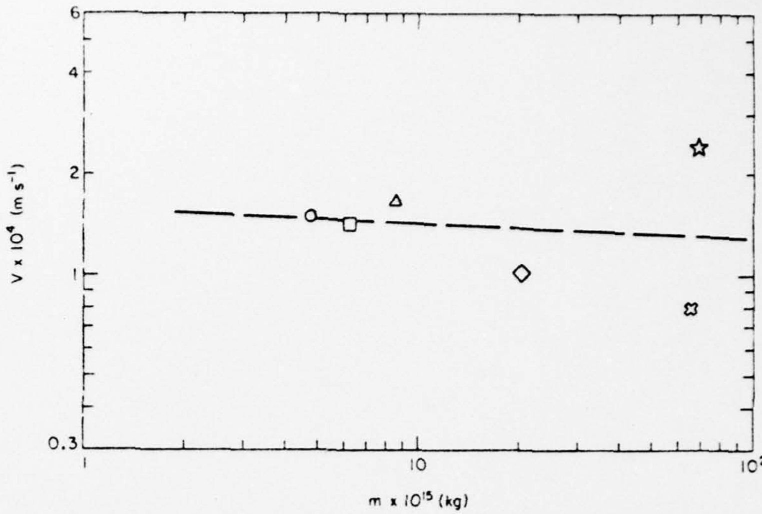

FIG. 3. Variation of swimming velocity of flagellates with their mass. The slope of the dotted regression line is −0·04. For other legends see caption to Fig. 2.

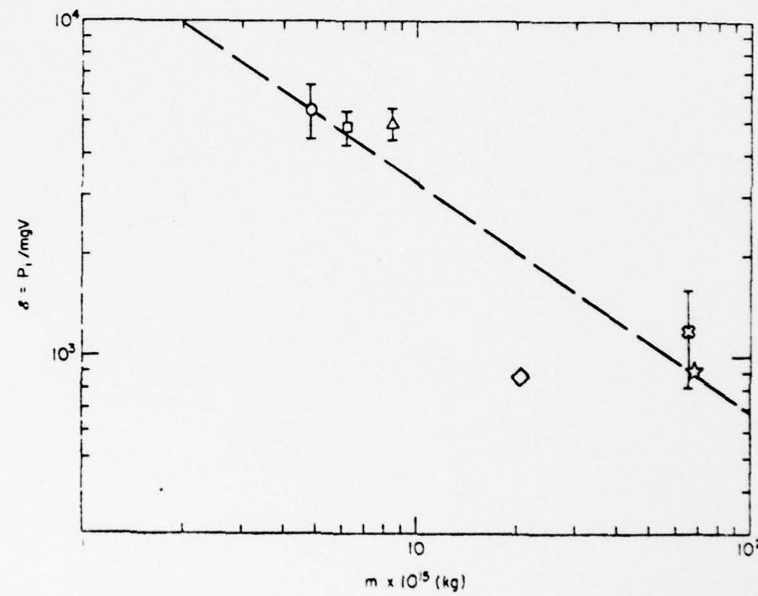

FIG. 4. The specific energy cost of flagellates versus their mass. The slope of the dotted regression lines is −0·68. For other legends see caption to Fig. 2.

and others for studies of comparative physiology. Figure 4 shows the specific energy cost of the six flagellates in question, which may be represented, by a least-square fit, as $\mathscr{E} = \text{const. } m^{-0.68}$. This $\mathscr{E}$–m relationship is quite similar to those of other aerial, aquatic and terrestrial animal groups, but the slope −0·68 of the regression line is steeper than most of them already known (see Tucker[65]).

Summarizing this preliminary study of flagellar propulsion, we have found

$$P_i \simeq \text{const. } m^{0.28}, \qquad V = \text{const. } m^{-0.04} \tag{19a}$$

and

$$\mathscr{E} = P_i/mg = \text{const. } m^{-0.68}. \tag{19b}$$

In view of the difficulties involved in such metabolism experiments, we should appreciate the value of these experimental results, although only six species have been studied, and not too much confidence can be placed in the quoted slopes of the regression lines. The results do throw enough light to make the following theoretical argument attractive.

Suppose we accept the assumptions that (i) the propulsive velocity V of a flagellum under the zero-thrust condition depends only on the wave form and beat frequency and is not appreciably affected by the presence of a cell body, and (ii) the power P_f required for maintaining a *steady* flagellar motion (hence P_f = const.) forms a basal reference above which the power P_b required for propelling the cell body (Eqn 17) will vary when the cell body size l_b is varied. Then the *changes* in the power input, P_i, would scale according to

$$P_i \propto l_b \propto m^{1/3}, \quad \text{and hence} \quad \mathscr{E} = P_i/mgV \quad \propto m^{-2/3}. \tag{20}$$

These relationships are in close agreement with (19a) and (19b). It will be of interest to acquire more experimental data for further studies along this line.

Ciliary Propulsion

Blake and Sleigh[13] and Holwill[34a,b] have given excellent surveys upon the mechanics and physiology of ciliary propulsion, and their introductory lectures on the subject at the 1974 Caltech Symposium were of especial value. They pointed out that ciliary length, pattern of movement and rate of beat are important factors in determining the effectiveness of propulsion of fluids by cilia, whether for ciliated protozoa or metazoa, or for the inner organs of higher animals. Ciliates are generally known as very impressive swimmers when judged by their specific speeds (body lengths travelled/s). However, the four types of metachronal pattern in which ciliary movements are organised

(symplectic, antiplectic, dexioplectic, and laeoplectic) are so different from each other that it would be inappropriate to study ciliary efficiency collectively, as these authors and others have pointed out. This is also true for studies of scaling problems in ciliary propulsion.

Theoretical analysis of ciliary propulsion began when Taylor[60] introduced the "envelope model", based on the idea that the concerted action of large numbers of cilia on the fluid can be represented by the waving motion of an impermeable inextensible sheet enveloping the cilia tips. This model has been extended to cover an extensible sheet, with an estimate of the inertia effect by Tuck,[62] and has been applied by Blake[10,11] to evaluate the motion of *Opalina*. It was pointed out by Lighthill[46] that it is only to symplectic motion that such a model should really be applied. In order to treat other types of metachronism, especially those such as antiplectic motion, in which the cilia tips may be far apart during the motion, Blake[12] developed a sublayer model in which each cilium was modelled by an elongated body attached to a flat cell surface.

Another simplified model, called the "traction-layer" model, has been investigated, at the suggestion of Wu,[77] by Keller.[39] It is based on the concept that the discrete forces of a system of cilia can be represented by an "equivalent" continuous distribution of an unsteady body force within the volume of the ciliary layer, provided that the spacings between adjacent cilia are small compared with the ciliary length, l_c. Conversion from the discrete to the continuum force is based on the resistive theory which gives the relationship between the original force exerted by a cilium, and its velocity relative to the flow produced by the ciliary system as a whole.

Using this procedure the model has been applied by Keller to an infinite plane ciliary layer with the body force represented by a Fourier series

$$f(x, y, t) = \sum_{n=0}^{N} f_n(y) \exp\left[in(kx - \omega t)\right] \qquad (-\infty < x < \infty, 0 < y < l_c) \tag{21}$$

where $N \leqslant \infty$, $\lambda = 2\pi/k$ is the metachronal wavelength, ω is the radian frequency, and f vanishes at the cell surface ($y = 0$) as well as outside the cilia layer ($y \geqslant l_c$). The functions $f_n(y)$ can be given a polynomial representation or be determined by numerical methods. The Stokes equation with this force term included can be solved to give the flow velocity for particular movements of the cilia. A related optimisation problem is to find the external mean force distribution $f_0(y)$ that will give the minimum power required, P_0, to maintain a rate of working on the fluid which is less than P_0 by a fixed amount; this is equivalent to finding the minimum power required for fixed mean square of f_0, averaged across the cilia layer. The result for a four-term polynomial representation of $f_0(y)$ is shown in Fig. 5. Thus we find the

mean flow velocity at the outer boundary of the cilia layer as

$$u_0(l_c) = 0{\cdot}52A(\omega l_c)(kl_c) = 0{\cdot}52Ac(2\pi l_c/\lambda)^2, \qquad (22)$$

where $c = \omega/k$ is the metachronal wave velocity and A is proportional to the amplitude of the dimensionless force distribution. The slope of $u_0(y)$ at $y = 0$ shows that there is a viscous skin friction at the cell surface which is counter-balanced by the fluid force acting on the cilia over the same area of the surface.

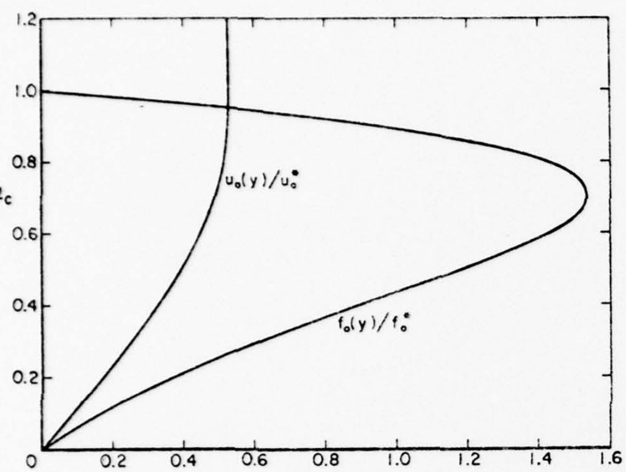

FIG. 5. The optimum continuous force distribution giving minimum power required for fixed mean square force, and the corresponding velocity profile. $f_0^* = A\mu\omega/k^2$ and $u_0^* = A\omega k l_c^2$ where l_c is the ciliary length, ω is the radian frequency and k the wave number of the ciliary wave, and A is a constant making the y-integral of $(f_0/f_0^*)^2$ unity.

The first harmonic velocity profile, $u_1(y)$, has been evaluated by Keller[39] in a few cases for which the wave parameters are available. The results for *Paramecium multimicronucleatum* are given in Fig. 6, from which we note that the contribution from the second harmonic is already very small. We further note from Fig. 6 that like the mean velocity $u_0(y)$, $u_1(y)$ is also proportional to $(kl_c)^2$, or $(l_c/\lambda)^2$.

Experimental investigation of the scaling relation (22) has not yet been fully carried out. Furthermore, a complete examination of the scaling of ciliary propulsion cannot be made without physiological data on the chemical energy input, which are also not yet available. In addition, the hydromechanical analysis must be carried out for a finite shape, in the manner indicated by Blake[10] and Brennen.[17]

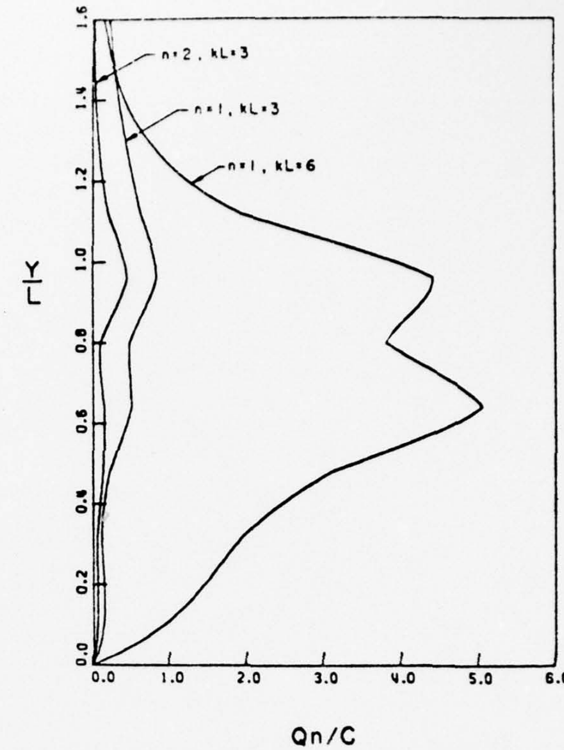

FIG. 6. Amplitude profile for the first and second harmonic x-components of flow velocity (Q_n, non-dimensionalised with respect to the metachronal wave speed $c = \omega/k$) for *Paramecium* with $ka = 0{\cdot}80$ and $kb = 1{\cdot}60$. (a and b are the row and column spacings between cilia, and L here denotes ciliary length).

LOCOMOTION OF LARGE AQUATIC ANIMALS

The swimming motions of large aquatic animals are characterized from the hydrodynamicist's point of view by large values of the ratio of typical inertial forces to typical viscous forces in the surrounding water, i.e. of the Reynolds number, $\mathrm{Re} = Vl/\nu \gg 1$. Here V is the mean swimming speed, l the length of the animal, and ν the coefficient of kinematic viscosity of the fluid. In general, the Reynolds number lies in the range $10^4 < \mathrm{Re} < 10^8$ for various fishes and cetaceans swimming normally. At such high Reynolds numbers the effects of viscosity are mostly confined to a thin boundary layer adjacent to the body surface. This is especially true for the streamlined body shapes of

such animals in undulatory swimming motion, when flow separation is not observed to occur, and only a very thin wake is formed behind the body. In such cases the boundary layer will continually grow with distance along the fish, but its maximum thickness (at the tail end) is generally not more than a few per cent of the body thickness. Viscous effects can therefore be neglected in analysing the flow outside this boundary layer. The pressures acting on the body are those predicted by inviscid theory, because the boundary layer is too thin to support a pressure gradient across it. These pressures generate a thrust force which must overcome the drag force in order to maintain a constant forward velocity. The drag force in this case arises mainly from the viscous shear stresses exerted by the fluid on the body surface; the contributions of "form drag" (resulting from the distal thickening of the boundary layer and possibly from flow separation), of "induced drag" (due to the shedding of vortex sheets), and of "wave resistance" (energy lost through making waves when swimming at the surface) are generally insignificant for these animals.

Thus the hydromechanical problem of fish locomotion can be conveniently divided into two parts: the drag of a streamlined body, analysed by calculating the viscous shear stresses in the boundary layer, and the generation of an equal and opposite thrust, determined from an analysis of the potential flow outside the boundary layer. *If the mean thrust is denoted by T, and the* mean drag force by D, we have, in steady swimming,

$$T = D. \tag{23}$$

Power Expenditure and Energy Balance

From the physical standpoint the minimum power necessary to transport the body at a given velocity V is determined by the resistance of the medium, the efficiency of the mode of locomotion, the energy consumption of the particular type of power plant that delivers the mechanical power, and many other factors. The principle of energy conservation may be expressed as

$$DV = \eta P, \tag{24}$$

which states that the animal's rate of working against the resistance D is provided by the power input P, used with efficiency η. For aquatic animals the variations of potential energy are generally unimportant, and in any case can be considered separately as for aerial and terrestrial animals.

The power input for locomotion can also be determined by measuring the animal's metabolic rate and by applying standard energy conversion factors. Thus, when P in Eqn (24) is taken to be the mechanical power, η is the hydrodynamic efficiency η_h of the propulsion. When P is taken instead to be the

...lic rate (the rate at which biochemical energy is released), then η ... to $\eta_h \eta_c$, where η_c is the efficiency with which biochemical energy is ...d to muscle power.

Metabolic Rate

The extensive literature on the metabolism and swimming speeds of fish makes it plain that the physical details of an experiment must be clearly specified, in order that its results may be interpreted correctly (see, for example) Winberg,[75] Drabkin[28] and Brett.[20, 21] Of major importance in the study of the metabolic rate of a fish are its level of activity and the temperature of the water (since water holds less dissolved oxygen at elevated temperatures). Such factors as preconditioning (a period of fasting and exercise prior to the test, so that none of the fish's energy is spent in digesting or absorbing food during the test), the state of maturity and sex of the specimen, and flow conditions during the experiment, are also important. We can give only a brief account here.

(i) *Level of Activity*

The level of activity in swimming fish is hard to characterize in general. However, for the salmon, a migratory fish, Brett[20, 21, 22] (see Fig. 7) found three levels of performance: sustained (speeds that can be maintained almost indefinitely), prolonged (speeds maintained for 1 or 2 hours with a steady effort, but leading to fatigue) and burst (speeds achieved at maximum effort lasting for only about 30 seconds). The physiological basis of each of these activity levels is different, and itself depends on body size and environmental temperature.

The relationship between swimming speed and metabolic rate can also be evaluated in terms of the rate of working by the muscle, as discussed in other lectures at this Symposium. Lighthill[47] reasoned that the efficiency with which muscles produce power increases in proportion to the frequency ω of contraction. Hence in both carangiform and lunate-tail swimming η_c should be proportional to the swimming velocity V. Thus, when the mechanical power required for maintaining the speed V is proportional to V^3, the fish consumes energy at a metabolic rate

$$P = P_b + \alpha V^2, \tag{25}$$

where P_b is its basal metabolic rate and α is a constant. It therefore follows that P/V, proportional to the specific energy cost $\mathscr{E}$ (Eqn 18), is given by

$$P/V = P_b/V + \alpha V, \tag{26}$$

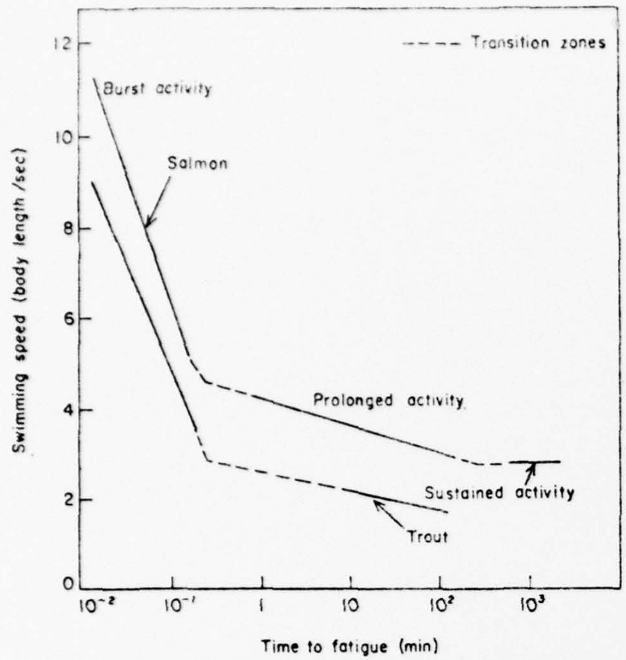

FIG. 7. Swimming endurance of sockeye salmon and rainbow trout. Transition zones between different levels of activity are shown with broken lines. (After Brett[19, 23]).

which has a minimum at the speed $V_m = (P_b/\alpha)^{1/2}$. A speed for which the specific energy cost is a minimum has been found by Brett[21] for salmon (see Fig. 8), by Tucker[64] for small parrots, and was also noted by Weihs[74] in his theoretical study. Figure 8 shows the basic curve of $\mathscr{E}$ against V for sockeye salmon; their ocean migrant speed is very close to the minimum energy cost, and their speeds in Fraser River migration ($\sim 1{\cdot}2\ \mathrm{m\,s^{-1}}$) are somewhat lower than their lowest burst speed.

(ii) *Fish Size and Metabolic Rate*

The relationship between body mass and the metabolic rate of fish has received considerable attention, particularly for the resting state (for expository reviews see Kleiber,[40] Schmidt-Nielsen[58]). The equation which describes this relationship is of the general form

$$P = am^b, \tag{27}$$

(see Eqn 19) or in the logarithmic form

$$\log P = \log a + b \log m, \tag{28}$$

where m is the body mass, and a and b are coefficients independent of body size. Gray[29] first tackled this problem by a different approach; he directly considered the total mass of muscle, m', so that $P = a'm'$, and derived the

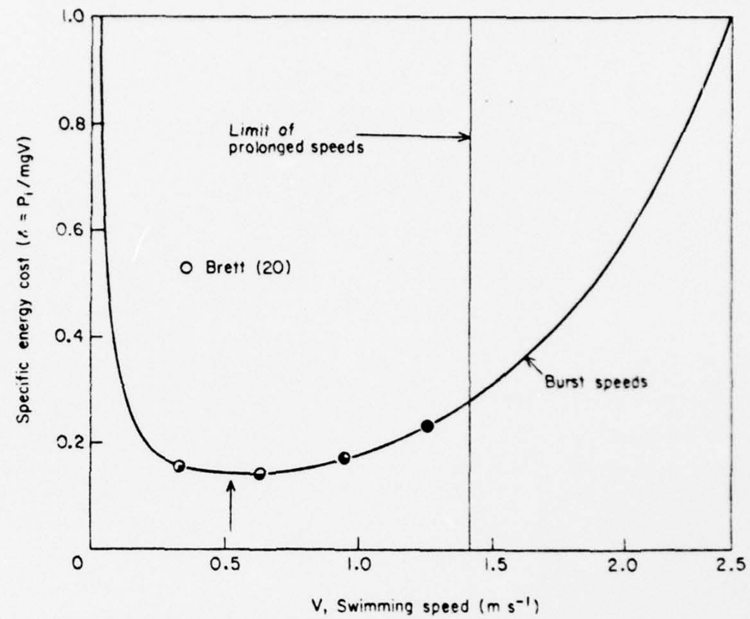

FIG. 8. Specific energy cost $\mathscr{E}$ as related to swimming speed, for adult sockeye salmon. Ocean migration occurs slightly above the speed at minimum $\mathscr{E}$ (shown with an arrow), which is about $\frac{1}{2}V_{crit}$(◉), while river migration takes place nearly at V_{crit}(●). For the definition of V_{crit} see text and the caption to Fig. 9. (Adapted from Brett[21, 23]).

power factor a' relating to unit mass of fish muscle from that of a rowing athlete. Application of this method by Bainbridge[2, 3, 4, 5] to several species of fish led to the equation $m' = 0{\cdot}005 l^{2{\cdot}9}$, where l is the length of the fish in cm when m' is measured in g.

Varous authors have considered body mass m directly. Winberg[75] examined 266 cases for freshwater fish and obtained an average value of $b = 0{\cdot}81$ (at 20°C). Heusner *et al.*[34] investigated three species and derived an overall mean of $b = 0{\cdot}73$ (at 25°C). There are other reports giving a rather wide range of values, varying all the way from near the "surface law" ($b = 0{\cdot}67$)

to direct proportionality ($b = 1$). The difficulty in seeking a generally applicable value seems to be associated with that met in measuring the drag of a fish.

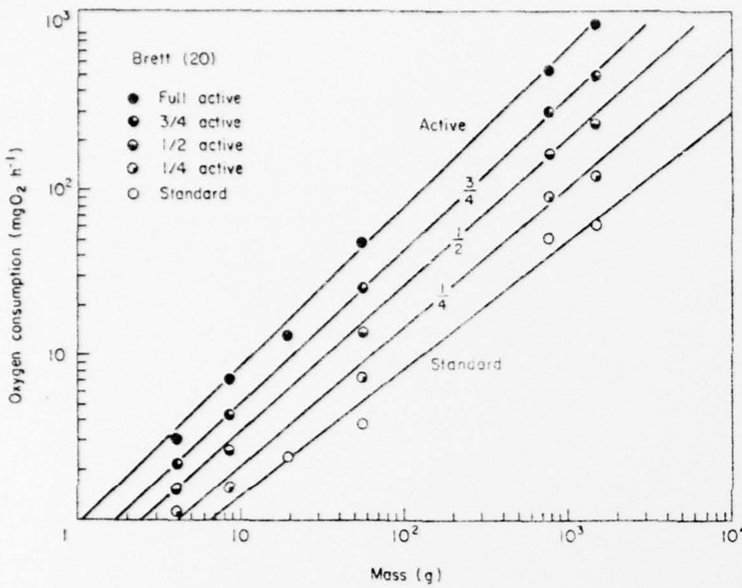

FIG. 9. Metabolic rate of sockeye salmon (*Oncorhunchus nerka*) as a function of body mass at various levels of swimming activity (15°C). The standard level was determined by extrapolation to zero swimming speed of the oxygen consumption vs. speed relation. The line at full activity corresponds to the maximum speed which could be sustained for 60 min, V_{crit}. Intermediate fraction levels correspond to swimming speeds equal to $\frac{3}{4}$, $\frac{1}{2}$, and $\frac{1}{4}$ of V_{crit} respectively.

Brett[18, 20, 21] has shed considerable and much-needed light on the problem by distinguishing between the different levels of activity. He provided the following results for the sockeye salmon (*Oncorhynchus nerka*), with oxygen consumption measured in mg O_2 h^{-1}, and body mass in g (see also Fig. 9):

$$\begin{aligned} \log a &= -0{\cdot}632 & b &= 0{\cdot}775 \pm 0{\cdot}145 \quad \text{(standard)} \\ &= -0{\cdot}523 & &= 0{\cdot}846 \pm 0{\cdot}145 \quad (\tfrac{1}{4}\ \text{max}) \\ &= -0{\cdot}357 & &= 0{\cdot}890 \pm 0{\cdot}145 \quad (\tfrac{1}{2}\ \text{max}) \\ &= -0{\cdot}223 & &= 0{\cdot}926 \pm 0{\cdot}145 \quad (\tfrac{3}{4}\ \text{max}) \\ &= -0{\cdot}050 & &= 0{\cdot}970 \pm 0{\cdot}053 \quad \text{(max)} \end{aligned} \tag{29}$$

Here the fractions are referred to the maximum speed which could be sustained for 60 min in fresh water at 15°C (V_{crit}), and his standard metabolic rate is obtained by extrapolating the O_2-consumption versus velocity curve to zero swimming velocity. This approach appears to make the study on the scaling of swimming velocity more systematic, as we now proceed to discuss.

Scaling of Swimming Velocity

In order to use the principles of dynamical similarity, we first express the drag D on a fish swimming at speed V in terms of its drag coefficient C_D, as follows:

$$D = \tfrac{1}{2}\rho V^2 S C_D \tag{30}$$

where ρ is the water density, S the fish surface area (proportional to l^2) and C_D depends on the Reynolds number Re and the body shape. Substitution of this expression and the metabolic rate relationship (27) into the energy equation (24) then yields

$$V^3 \propto l^{3b-2}/C_D. \tag{31}$$

Two cases can be examined by assuming that for carangiform and lunate-tail swimming, in both of which the fish is well-streamlined, C_D is the same, apart from a shape factor, as that of a flat plate of the same area at the same Reynolds number. That is, C_D is proportional to $\mathrm{Re}^{-1/2}$ or $\mathrm{Re}^{-1/5}$ according as the boundary layer is laminar or turbulent. This leads to the scaling law:

$$V = \text{const.}\ l^{\beta}, \tag{32}$$

with

$$\begin{aligned} \beta &= \tfrac{3}{5}(2b-1) \quad \text{(laminar)} \\ \beta &= \tfrac{3}{14}(5b-3) \quad \text{(turbulent)} \\ \beta &= b - \tfrac{2}{3} \qquad (C_D = \text{const.}) \end{aligned}$$

The last case (of quite large but constant C_D) corresponds to the situation

TABLE I

C_D \ β \ b	0·78 (standard)	0·85 ($\frac{1}{4}$-max)	0·89 ($\frac{1}{2}$-max)	0·93 ($\frac{3}{4}$-max)	0·97 (max)	1·00
laminar	0·33	0·42	0·47	0·51	0·56	0·60
turbulent	0·19	0·26	0·31	0·35	0·40	0·43
C_D = const.	0·11	0·18	0·22	0·26	0·30	0·33

for separated flow past a blunt body with a broad wake formation, or to the case when flow separation occurs in the cross-flow past an undulating fish body. If Brett's values for b are adopted we obtain Table I for β. The last column, for $b = 1$, is included to show the values of the index β when the metabolic rate is proportional to body weight, and the last row, for C_D = const., is for the hypothetical case in which the flow is fully separated.

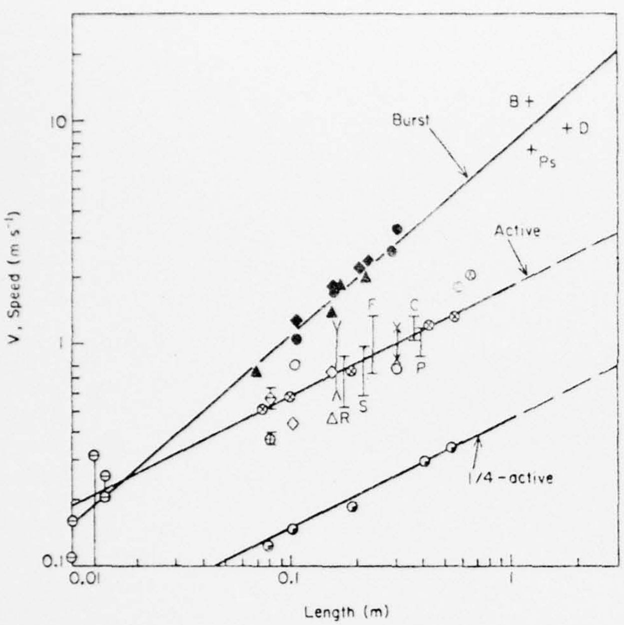

FIG. 10. Variation of swimming speed with body length at different levels of activity. *Burst speed data*: ◆ dace, ▲ goldfish, ● trout, B+ barracuda, P_s + porpoise, D + dolphin (Bainbridge[5]). *Full activity data*: open symbols (Bainbridge[5]); ⊗ sockeye salmon (15°C) (Brett[20]); bass, ⊕ coho salmon (Dahlberg *et al.*[27]); C cod, R redfish, F winter flounder, S sculpin, P pout (Beamish[9]); goldfish (Smit *et al.*[59]); ⊖ larval anchovy (Hunter[36]); ×—× herring (Jones[38]); salmon, trout (Paulick and DeLacy[55]). $\frac{1}{4}$-*activity data*: sockeye salmon at 15°C (Brett[20]).

A collection of existing experimental data is given in Fig. 10. In the log V vs log l plot for (i) Brett's 60-min. maximum activity results for salmon at 15°C, (ii) Beamish's[9] results for 6 species of fish over a range of temperatures (8–14°C) and endurance spans, and (iii) a few other sources (see Fig. 10 caption), the slope of the mean regression line is 0·5 (i.e. $\beta = 0{\cdot}5$). This result led Brett[20, 21] to propose "that the swimming speed is proportional to $l^{0\cdot5}$,

indicating a decrease in the relative ability to maintain a sustained speed as size increases". It is of interest to point out that the speed at the $\frac{1}{4}$-max activity level ($b = 0{\cdot}85$) of the sockeye salmon is also proportional to $l^{0\cdot5}$ (see Fig. 10). There are, however, other reports (Brett,[22] Magnuson,[50] Hunter,[35] Hunter and Zweifel[37]) indicating that a better overall average value for β is 0·6.

Considerable attention has been given to the burst speeds which, for various species of streamlined fish, tend to be nearly independent of both size and temperature. A representative plot is included in Fig. 10, showing Bainbridge's[5] results for 4 species of fish and two cetaceans; the slope of this line gives a value of β equal to 0·88. Similar values have been obtained by others, such as $\beta = 0{\cdot}94$ for herring (at $\sim 12°$C) by Blaxter and Dickson.[16] In fact, a speed of 10 lengths per second has been regarded by several authors as a "common rule" for the maximum burst speed of many streamlined fish.

At this point a comparison between experiment and the foregoing similitude calculation may have far-reaching implications. First, on the basis of the observed sustained speeds (with the index $\beta = 0{\cdot}5$) and the corresponding metabolic-rate index $b = 0{\cdot}97$, it may be argued by implication (see the fourth column of Table I) that the boundary layer adjacent to the *swimming* fish would be at most only partially turbulent up to Reynolds number of 10^6 (the upper range covered by the data). Furthermore, there is no evidence to suggest any flow separation. If this argument can be established, the study of the metabolism of swimming fish will yield most valuable results for hydrodynamicists, and may enable them to overcome the difficulties in making measurements in the boundary layer over an undulating body and hence estimating the drag force. Further, we note that the rule of burst-speed = $10\,l\,s^{-1}$ would correspond to a value of b equal to 1·33 (for laminar boundary layers), and even higher values when the flow is turbulent. Whether this implies a substantial depletion of stored energy or whether it has some other significance remains to be explored.

Specific Energy Cost

The results obtained above for the scaling of metabolic rate and swimming velocity may now be used to evaluate the scaling of the specific energy cost, $\mathscr{E} = P/mgV$. From (18), (27) and (32) we immediately deduce that

$$\mathscr{E} = P/mgV = \text{const. } m^{-\gamma} \tag{33}$$

where

$$\gamma = 1 - b + \beta/3. \tag{34}$$

Using Table I we obtain for γ the following result (Table II):

TABLE II.

C_D \ b (γ)	0·78 (standard)	0·85 ($\frac{1}{4}$-max)	0·89 ($\frac{1}{2}$-max)	0·93 ($\frac{3}{4}$-max)	0·97 (max)	1·00
laminar	0·34	0·30	0·27	0·24	0·22	0·20
turbulent	0·29	0·24	0·21	0·19	0·16	0·14
C_D = const.	0·26	0·21	0·18	0·16	0·13	0·11

Figure 11 presents the experimental data, derived from those given in Figs 9 and 10, showing how the specific energy cost varies with body size for fish swimming at different levels of activity. The solid lines are regression lines obtained by a least-square-error fit, giving $\gamma = 0{\cdot}34$ at $\frac{1}{4}$-max, 0·29 at $\frac{1}{2}$-max, 0·25 at $\frac{3}{4}$-max, and 0·21 at full activity. These values of γ and the observed mean of $\beta = 0{\cdot}5$ are plotted against b (which may be regarded as a measure of the level of activity) in Fig. 12. Also shown are the similarity predictions of β and γ given by (32) (or Table I) and (34) (or Table II) for the three distinct reference states characterized by a laminar boundary layer, a turbulent boundary layer and separated cross flow. This comparison

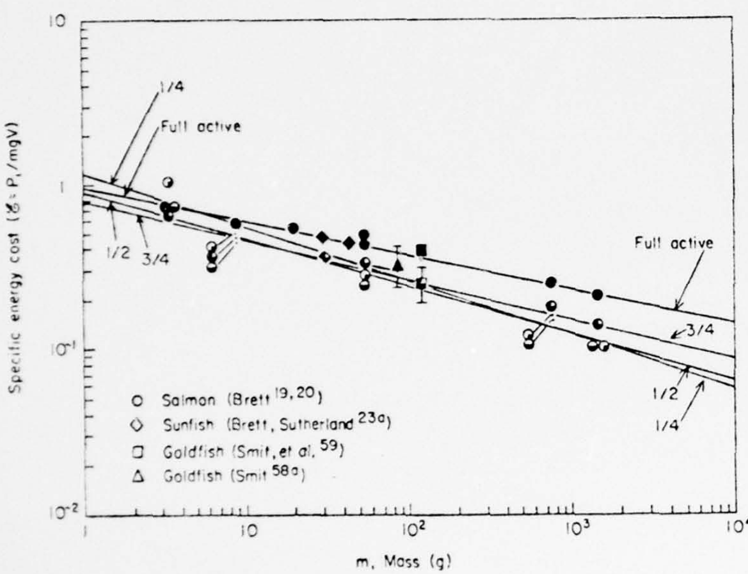

FIG. 11. Relation between specific energy cost $\mathscr{E}$ and body size for fish swimming at different levels of activity. Solid lines are regression lines obtained from data of Brett[20] for salmon at 15°C. For other legend and symbols see Fig. 9.

strongly suggests that the boundary layers of these swimming fish would be largely laminar at these high Reynolds numbers ($8 \times 10^3 < \mathrm{Re} < 1{\cdot}4 \times 10^6$ being the range covered by the test cases), with at most only a small (presumably distal) part turbulent, and that the specimens tested were swimming at somewhere about $\frac{3}{4}$ of their maximum sustainable activity.

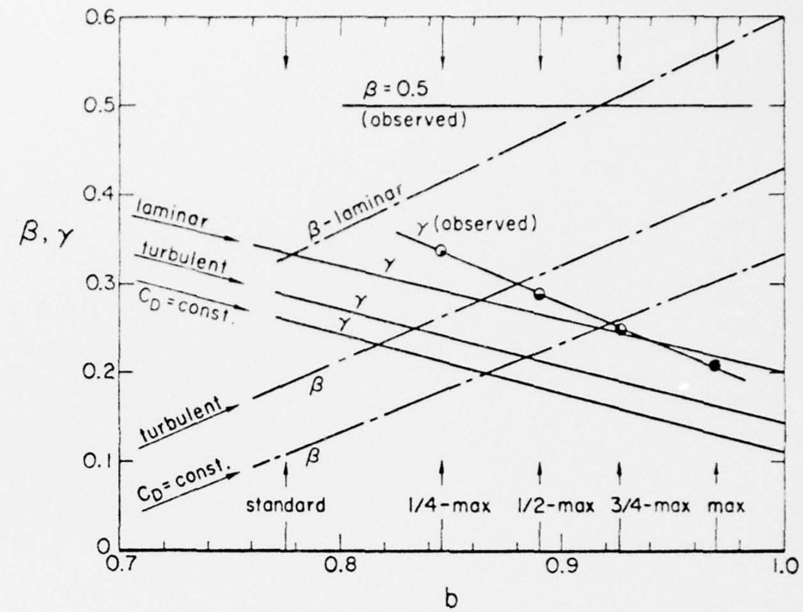

FIG. 12. Comparison of the observed values of β (Brett[20, 21]) and γ (see Fig. 11) with the similartiy predictions (Eqs (32), (34)) based on the three distinct reference states characterized by a laminar boundary layer, a turbulent boundary layer and C_D = const. (for the case of separated cross flows).

The specific energy cost of transport has also been discussed in the recent studies of Schmidt-Nielsen[57] and Tucker[65] for the locomotion of various animals. For comparison we find, from Schmidt-Nielsen's Fig. 1(a) and Tucker's Fig. 2, that the observed values of γ for fish are

$$\gamma = 0{\cdot}30 \qquad \text{(Schmidt-Nielsen)}, \tag{35}$$

$$\gamma = 0{\cdot}27 \qquad \text{(Tucker)}. \tag{36}$$

These values of γ are in accord with the present finding when the level of activity lies between about $\frac{1}{2}$ and $\frac{3}{4}$ of the maximum performance.

With particular reference to fish size we note from Fig. 11 that the regression lines of $\bar{\delta}$ at different levels of activity cross each other at a certain mass. This cross-over suggests that some (specific) energy would be saved if smaller fish were to swim at speeds corresponding to greater activity and larger fish were to cruise at lower relative speeds.

Scaling of Tail Beat Frequency and Body Wavelength

Bainbridge[2, 4, 7] observed that the maximum amplitude of the tail beat of fishes in carangiform motion is approximately 0·2 of the fish length l, with no noticeable dependence on other parameters. The "reduced frequency" $\omega l/V$, where ω is the radian frequency, is scale independent, and takes values around 10. Observations by other authors are essentially in agreement with Bainbridge's. According to Hunter and Zweifel,[37] however, the reduced frequency of jack mackerel was found to decrease slightly with increasing size (with a mean value of $\omega l/V$ equal to 11 for $l = 4{\cdot}5$ cm, decreasing to 7·44 for $l = 27$ cm), while the amplitude remains constant about the value of 0·23 l.

A theoretical estimate of the scaling of ω can be obtained by applying slender-body theory (Lighthill,[42] Wu,[76] Newman and Wu[53] and Newman[52]) which provides the following approximate relation for the mean thrust

$$T \propto \rho b_0^2 \omega^2 a_0^2 (1 - V/c), \tag{37}$$

where a_0 represents the amplitude of oscillation of the fish tail, b_0 its characteristic depth, and $c = \omega/k = f\lambda$ denotes the wave velocity of the wave (of frequency f and wavelength λ) which is propagated distally along the body. The dimensionless coefficient multiplying (37) is either constant or very nearly scale-independent. If we assume that c/V (or, equivalently, the hydromechanical efficiency) is scale-independent, equating T and the drag D (see Eqn 23) yields

$$\omega l/V = \text{const.}\, C_D^{1/2} \tag{38}$$

in which we have taken a_0 and b_0 to be proportional to l and S to l^2. Thus, for laminar flow, with V proportional to $l^{1/2}$ (see Eqn 32 and its sequel), we obtain

$$\omega l/V = \text{const.}\, l^{-3/8}. \tag{39}$$

Though this estimate is somewhat crude, it is in qualitative accord with the observed data of Hunter and Zweifel. (The scaling of $\omega l/V$ would be weaker than $l^{-3/8}$ for smaller $\beta < 0{\cdot}5$). The corresponding scaling of ω is

$$\omega = \text{const.}\, l^{-7/8} = \text{const.}\, l^{-0{\cdot}88}. \tag{40}$$

Further, if c/V is again assumed to be scale-independent (which implies that the hydromechanical efficiency is likewise scale-independent), it then follows that the wavelength λ will scale as

$$\lambda = c/f = (V/fl)(c/V)l = \text{const.}\, l^{11/8}. \tag{41}$$

It should be of interest to examine these scaling relations when the necessary data are available.

In passing we note that the wing beat frequency of many species of birds tends to be proportional to $m^{-0{\cdot}6}$ or to $l^{-0{\cdot}78}$ (Greenewalt,[32] Alexander (Ref. 1, p. 7)) which is quite close to the expression (40) for fish.

Viscous Resistance

As we noted earlier, reasonable accuracy in the measurement of metabolic-rate, coupled with direct observations of pertinent parameters such as the fish mass, length, swimming velocity, and the frequency and wavelength of its tail beat, has enabled us not only to carry out the similarity study but also yields valuable information about the drag coefficient. This information appears to contain indirect evidence concerning both the functional dependence of C_D on the Reynolds number Re and, even, its order of magnitude, which in turn may throw light on whether there is transition from laminar to turbulent flow in the boundary layer and on the possible occurrence of flow separation in unsteady flows. To acquire such information by direct measurement for freely swimming fish has proved too difficult a task, and it is worth commenting on this.

The great difficulties involved in measuring the drag on a swimming fish directly has forced researchers to assume that it is the same as the drag on an equivalent straight rigid body. Therefore many attempts have been made to measure the viscous drag of either a mechanical model, or a paralyzed or pickled fish, in steady flow in wind or water-tunnels, towing tanks, or water tanks for drop-down tests; another approach has been to observe the retardation of a fish in glide (for brief reviews see Gray[30a], Newman and Wu[53]). Generally speaking, the measured values of the drag coefficient C_D show wide scatter over a range of a few times to tens of times the drag coefficient for turbulent skin friction on a flat plate of the same area at the same Reynolds number. However, there are reports (Lang and Daybell[41], Webb[73]) indicating that the measured drag is close to that of an equivalent mechanical model. Drastic improvement in experimental accuracy is urgently needed, but difficult to achieve.

I would like to remark that the basic assumption on the equivalence of swimming drag to model drag may not be generally valid. This is because the pressure field around a swimming fish must differ considerably from that

about a rigid model, and this difference will fundamentally alter the boundary layer calculation. At an appropriate frequency and phase, the undulatory motion may delay both the transition to turbulence and the flow separation.

CONCLUSION

In the field of aquatic animal locomotion the number of groups of animals which are fundamentally distinct, from either the hydromechanical or the physiological point of view, has been placed by Lighthill[43] to be about 10. The Reynolds numbers achieved in their locomotion span the range from 10^{-6} for eukaryotic flagella to about 10^8 for the giant blue whale. The different modes of propulsion include the flagellar and ciliary wave motions of protozoa, the undulatory movements in anguilliform, carangiform and lunate-tail swimming of many fish, the flying mode adopted by rays, turtles and penguins, the jet propulsion of squids, and so forth. Equally vast in variety are their distinct physiological characteristics and behavior. Nevertheless, by studying the different scaling problems some quite definite relations between the key parameters have emerged, and these seem to exhibit certain underlying principles. The field is extremely complex, and I have concentrated on only a few points where the problems are relatively easy, and have pointed out some hopeful possibilities for the future. I am quite sure that the conspicuous gaps which I have left in my discussion will be closed by other speakers with their enlightening observations. May I reiterate my conviction that collaborative studies in this multidisciplinary subject can be surprisingly rewarding.

ACKNOWLEDGMENT

I would like to express my deep gratitude to Professor Charles Brokaw, Dr Allan Chwang, Dr Howard Winet, Dr Anthony Cheung, and Mr George Yates not only for the extremely valuable discussions I have had with them, but also for their splendid support in providing me with important knowledge and material throughout the course of preparation of this work. I am also most thankful to Helen Burrus for her experienced assistance in many ways.

This work was jointly sponsored by the Office of Naval Research and the National Science Foundation. Their continuous support is gratefully acknowledged.

REFERENCES

1. Alexander, R. McNeill. "Size and Shape". Studies in Biology No. 29. Edward Arnold Ltd., London (1971).
2. Bainbridge, R. The speed of swimming of fish as related to size and to the frequency and amplitude of the tail beat. *J. exp. Biol.* **35**, 109–133 (1958a).
3. Bainbridge, R. The locomotion of fish. *New Scient.* **4**, 476–478 (1958b).
4. Bainbridge, R. Speed and stamina in three fish. *J. exp. Biol.* **37**, 129–153 (1960).
5. Bainbridge, R. Problems of fish locomotion. *In* "Vertebrate Locomotion", (Harrison, J. E., ed.), *Symp. Zool. Soc. Lond.* **5**, 13–32 (1961).
6. Bainbridge, R. Training, speed and stamina in trout. *J. exp. Biol.* **39**, 537–555 (1962).
7. Bainbridge, R. Caudal fin and body movement in the propulsion of some fish. *J. exp. Biol.* **40**, 23–56 (1963).
8. Batchelor, G. K. Slender-body theory for particles of arbitrary cross-section in Stokes flow. *J. Fluid Mech.* **44**, 419–440 (1970).
9. Beamish, F. W. H. Swimming endurance of some northwest Atlantic fishes. *J. Fish. Res. Board Can.* **23**, 341–347 (1966).
10. Blake, J. R. A spherical envelope approach to ciliary propulsion. *J. Fluid Mech.* **46**, 199–208 (1971a).
11. Blake, J. R. Infinite model for ciliary propulsion. *J. Fluid Mech.* **49**, 209–222 (1971b).
12. Blake, J. R. A model for the micro-structure in ciliated organisms. *J. Fluid Mech.* **55**, 1–23 (1972).
13. Blake, J. R. and Sleigh, M. A. Mechanics of ciliary locomotion. *Biol. Rev.* **49**, 85–125 (1974).
14. Blake, J. R. and Sleigh, M. A. Hydromechanical aspects of ciliary propulsion. *In* "Swimming and Flying in Nature". Plenum Publ., New York (1975).
15. Blaxter, J. H. S. Swimming speeds of fish. *FAO Fish. Rep.* 62, **2**, 69–100 (1967).
16. Blaxter, J. H. S. and Dickson, W. Observations on the swimming speeds of fish. *J. Cons. Int. Explor. Mer.* **24**, 474–479 (1959).
17. Brennen, C. An oscillating-boundary-layer theory for ciliary propulsion. *J. Fluid Mech.* **65**, 799–824 (1974).
18. Brett, J. R. The energy required for swimming by young sockeye salmon with a comparison of the drag force on a dead fish. *Trans. R. Soc. Can.* **1**, Sec. IV, 441–457 (1963).
19. Brett, J. R. The respiratory metabolism and swimming performance of young sockeye salmon. *J. Fish Res. Board Can.* **21**, 1183–1226 (1964).
20. Brett, J. R. The relation of size to the rate of oxygen consumption and sustained swimming speeds of sockeye salmon (*Oncorhynchus nerka*). *J. Fish. Res. Board Can.* **22**, 1491–1501 (1965a).
21. Brett, J. R. The swimming energetics of salmon. *Sci. Am.* **213**, 80–85 (1965b).
22. Brett, J. R. Swimming performance of sockeye salmon (*Oncorhynchus nerka*) in relation to fatigue time and temperature. *J. Fish. Res. Board Can.* **24**, 1731–1741 (1967a).
23. Brett, J. R. "Salmon". *In* "Encyclopaedia of Science and Technology" McGraw-Hill. 348–349 (1967b).

23a Brett, J. R. and Sutherland, D. B. Respiratory metabolism of Pumpkinseed (*Lepomis gibbosus*) in relation to swimming speed. *J. Fish. Res. Board Can.* **22**, 405–409 (1965).

24. Brokaw, C. J. and Gibbons, I. R. Mechanisms of movement in simple flagella and cilia. *In* "Swimming and flying in Nature". Plenum Publ., New York (1975).
25. Chwang, A. T. and Wu, T. Y. A note on the helical movement of micro-organisms. *Proc. R. Soc. Lond.* **B178**, 327–346 (1971).
26. Cox, R. G. The motion of long slender bodies in a viscous fluid. Part 1. General theory. *J. Fluid Mech.* **44**, 791–810 (1970).
27. Dahlberg, M. L., Shumway, D. L. and Doudonoff, P. Influence of dissolved oxygen and carbon dioxide in the swimming performance of large-mouthed bass and coho salmon. *J. Fish. Res. Board Can.* **25**, 49–70 (1968).
28. Drabkin, D. L. Imperfection: Biochemical phobias and metabolic ambivalence. *Perspectives Biol. Med.* **2**, 473–517 (1959).
29. Gray, J. Studies in animal locomotion. *J. exp. Biol.* **13**, 192–199 (1936).
30. Gray, J. How fish swim. *Sci. Am.* **197**, 48–54 (1957).
30a Gray, J. "Animal Locomotion". Weidenfeld and Nicolson, London (1968).
31. Gray, J. and Hancock, G. J. The propulsion of sea-urchin spermatozoa. *J. exp. Biol.* **32**, 802–814 (1955).
32. Greenewalt, C. H. Dimensional relationships for flying animals. *Smithson Misc. Collns.* **144**(2), 1–46 (1962).
33. Hancock, G. J. The self-propulsion of microscopic organisms through liquids. *Proc. R. Soc. Lond.* **A127**, 96–121 (1953).
34. Heusner, A., Kayser, C., Marx, C., Stussi, T. and Harmelin, M. L. Relation entre le poids et la consommation d'oxygene. II. Etude intraspecifique chez le poisson. *C.R. Soc. Biol.* **157**(3), 654 (1963).
34a Holwill, M. E. J. Hydrodynamic aspects of ciliary and flagellar movement. Chapt. 8 in "Cilia and Flagella", (M. A. Sleigh, ed.), 143–175. Academic Press, New York (1974).
34b Holwill, M. E. J. The role of body oscillation in the propulsion of micro-organisms. *In* "Swimming and Flying in Nature". Plenun Publ., New York (1975).
35. Hunter, J. R. Sustained speed of jack mackerel. *Fish. Bull.* **69**, 267–271 (1971).
36. Hunter, J. R. Swimming and feeding behaviour of larval anchovy *Engraulis mordax*. *Fish. Bull.* **70**, 821–838 (1972).
37. Hunter, J. R. and Zweifel, J. R. Swimming speed, tail beat frequency, tail beat amplitude and size in jack mackerel, *Trachurus symmetricus* and other fishes. *Fish. Bull.* **69**, 253–266 (1971).
38. Jones, D. J. Theoretical analysis of factors which may limit the maximum oxygen uptake of fish. *J. theor. Biol.* **32**, 341–349 (1971).
39. Keller, S. R. "Fluid Mechanical Investigations of Ciliary Propulsion". Ph.D. Thesis, Calif. Inst. of Technology, Pasadena, Calif. (1975).
40. Kleiber, M. Prefatory chapter: An old professor of animal husbandry ruminates. *Ann. Rev. Physiol.* **29**, 1–20 (1967).
41. Lang, T. G. and Daybell, D. A. Porpoise performance tests in a seawater tank. NAVWEPS Rep. 8060, NOTS TP 3063. Naval Ordnance Test Station, China Lake, Calif. (1963).
42. Lighthill, M. J. Note on the swimming of slender fish. *J. Fluid Mech.* **9**, 305–317 (1960).
43. Lighthill, M. J. Hydromechanics of aquatic animal propulsion. *Ann. Rev. Fluid Mech.* **1**, 413–445 (1969).
44. Lighthill, M. J. Aquatic animal propulsion of high hydromechanical efficiency. *J. Fluid Mech.* **44**, 265–301 (1970).

45. Lighthill, M. J. Large-amplitude elongated-body theory of fish locomotion. *Proc. R. Soc. Lond.* **B179**, 125–138 (1971).
46. Lighthill, M. J. "Aquatic animal locomotion". *In* Proc. 13th Intern. Congr. IUTAM (August, Moscow). Springer Verlag, Berlin (1972).
47. Lighthill, M. J. Scaling problems in aquatic locomotion. Symposium at the Duke University, 1973 (unpublished).
48. Lighthill, M. J. "Mathematical Biofluiddynamics", SIAM, Philadelphia (1975).
49. Lighthill, M. J. Flagellar hydrodynamics. The John von Neumann Lecture, *SIAM Reviews*, 1975.
50. Magnuson, J. J. Hydrostatic equilibrium of *Euthynnus affinis*, a pelagic teleost without a gas bladder. *Copeia*, 56–85 (1970).
51. Magnuson, J. J. Comparative study of adaptations for continuous swimming and hydrostatic equilibrium of scombroid and xiphoid fishes. *Fish. Bull.* **71**, 337–356 (1973).
52. Newman, J. N. The force on a slender fish-like body. *J. Fluid Mech.* **58**, 689–702 (1973).
53. Newman, J. N. and Wu, T. Y. A generalized slender-body theory for fish-like forms. *J. Fluid Mech.* **57**, 673–693 (1973).
54. Newman, J. N. and Wu, T. Y. Hydromechanical aspects of fish swimming. *In* "Swimming and Flying in Nature". Plenum Publ., New York (1975).
55. Paulick, G. J. and DeLacy, A. C. Swimming ability of upstream migrant silver salmon, sockeye salmon and steelhead at several water velocities. Univ. Wash. Coll. Fish. Tech. Rep. 44 (1957).
56. Schmidt-Nielsen, K. Energy metabolism, body size, and problems of scaling. *Fed. Proc.* **29** (4), 1524 (1970).
57. Schmidt-Nielsen, K. Locomotion: Energy cost of swimming, flying, and running. *Science*, **177**, 222–228 (1972a).
58. Schmidt-Nielsen, K. "How Animals Work". Cambridge University Press (1972b).
58a Smit, H. Some experiments on the oxygen consumption of goldfish (*Carassius auratus* L) in relation to swimming speed. *Can. J. Zool.* **43**, 623–633 (1965).
59. Smit, H., Amelink-Houtstaal, J. M., Vijverberg, J. and von Vaupel-Klein, J. C. Oxygen consumption and efficiency of swimming goldfish. *Comp. Biochem. Physiol.* **39A**, 1–28 (1971).
60. Taylor, G. I. Analysis of swimming of microscopic organisms. *Proc. R. Soc. Lond.*, **A209**, 447–461 (1951).
61. Tillet, J. P. K. Axial and transverse Stokes flow past slender axisymmetric bodies. *J. Fluid Mech.* **44**, 401–417 (1970).
62. Tuck, E. O. A note on a swimming problem. *J. Fluid Mech.* **31**, 305–308 (1968).
63. Tucker, V. A. Energetic cost of locomotion in animals. *Comp. Biochem. Physiol.* **34**, 841–846 (1970).
64. Tucker, V. A. Aerial and terrestrial locomotion: A comparison of energetics. In Bolis, L., Schmidt-Nielsen, K. and Maddrell, S. H. P. (eds.), "Comparative Physiology", North-Holland (1973).
65. Tucker, V. A. The energetic cost of moving about. *Am. Scientist*, **63**, No. 4, 413–419 (1975).
66. von Karman, Th. and Gabrielli, G. What price speed? Specific power required for propulsion of vehicles. *Mech. Engng.* **72**, 775–781, 1950 Thurston Lecture (Collected works of Theodore von Karman, IV, 399–414) (1950).

67. Webb, P. W. "Some Aspects of the Energetics of Swimming of Fish with Special Reference to the Cruising Performance of Rainbow Trout" Ph.D. Thesis, Univ. Bristol, Bristol, England (1970).
68. Webb, P. W. The swimming energetics of trout. I. Thrust and power output at cruising speeds. *J. exp. Biol.* **55**, 489–520 (1971a).
69. Webb, P. W. The swimming energetics of trout. II. Oxygen consumption and swimming efficiency. *J. exp. Biol.* **55**, 521–540 (1971b).
70. Webb, P. W. Effects of partial caudal-fin amputation on the kinematics and metabolic rate of underyearling sockeye salmon (*Oncorhynchus nerka*) at steady swimming speed. *J. exp. Biol.* **59**, 565–581 (1973a).
71. Webb, P. W. Kinematics of pectoral fin propulsion in *Cymatogaster aggregata. J. exp. Biol.* **59**, 697–710 (1973b).
72. Webb, P. W. Pisces (zoology) bioenergetics. McGraw-Hill, Encycl. Sci. Technol. Yearb. 1973, 333–336 (1974).
73. Webb, P. W. Hydrodynamics and energetics of fish propulsion. Bulletin 190, Fish. Res. Board. Can., Ottawa, Canada (1975).
74. Weihs, D. Mechanically efficient swimming techniques for fish with negative buoyancy. *J. Marine Res.* 31, 194–209 (1973).
75. Winberg, G. G. Rate of metabolism and food requirements of fishes. Bylorussian State University. Minsk 251 p. (Transl. Fish. Res. Bd. Canada, No. 194) (1956).
76. Wu, T. Y. Hydromechanics of swimming propulsion. Part 3. Swimming and optimum movements of slender fish with side fins. *J. Fluid Mech.* **46**, 545–568 (1971).
77. Wu, T. Y. Fluid mechanics of ciliary propulsion. Proc. 10th Anniv. Meeting Soc. Eng. Sci., North Carolina State U. Raleigh, North Carolina (1973).

DISTRIBUTION LIST FOR UNCLASSIFIED
TECHNICAL REPORTS ISSUED UNDER
CONTRACT N00014-76-C-0157 TASK NR 062-230

All addressees receive one copy unless otherwise specified

Defense Documentation Center
Cameron Station
Alexandria, VA 22314 12 copies

Technical Library
David W. Taylor Naval Ship Research
and Development Center
Annapolis Laboratory
Annapolis, MD 21402

Professor Bruce Johnson
Engineering Department
Naval Academy
Annapolis MD 21402

Library
Naval Academy
Annapolis, MD 21402

Professor R. B. Couch
Department of Naval Architecture
and Marine Engineering
University of Michigan
Ann Arbor, MI 48105

Professor T. Francis Ogilvie
Department of Naval Architecture
and Marine Engineering
University of Michigan
Ann Arbor, MI 48105

Professor C. S. Yih
Department of Engineering Mechanics
University of Michigan
Ann Arbor, MI 48105

Dr. Coda Pan
Shaker Research Corporation
Northway 10 Executive Park
Ballston Lake, NY 12019

Professor O. M. Phillips
Department of Earth and Planetary
Sciences
The Johns Hopkins University
Charles and 34th Street
Baltimore, MD 21218

NASA Scientific and Technical Information
Facility
P. O. Box 8757
Baltimore/Washington International Airport
Maryland 21240

Librarian
Department of Naval Architecture
University of California
Berkeley, CA 94720

Professor P. Naghdi
College of Mechanical Engineering
University of California
Berkeley, CA 94720

Professor J. R. Paulling
Department of Naval Architecture
University of California
Berkeley, CA 94720

Professor W. C. Webster
Department of Naval Architecture
University of California
Berkeley, CA 94720

Professor J. V. Wehausen
Department of Naval Architecture
University of California
Berkeley, CA 94720

Director
Office of Naval Research Branch Office
495 Summer Street
Boston, MA 02210

Commander
Puget Sound Naval Shipyard
Bremerton, WA 98314

Dr. Alfred Ritter
CALSPAN Corporation
P. O. Box 235
Buffalo, NY 14221

Professor G. Birkhoff
Department of Mathematics
Harvard University
Cambridge, MA 02138

Professor G. F. Carrier
Division of Engineering and
Applied Physics
Pierce Hall
Harvard University
Cambridge, MA 02138

Professor M. A. Abkowitz
Department of Ocean Engineering
Massachusetts Institute of Technology
Cambridge, MA 02139

Commanding Officer
NROTC Naval Administrative Unit
Massachusetts Institute of Technology
Cambridge, MA 02139

Professor P. Leehey
Department of Ocean Engineering
Massachusetts Institute of Technology
Cambridge, MA 02139

Professor Phillip Mandel
Department of Ocean Engineering
Massachusetts Institute of Technology
Cambridge, MA 02139

Professor C. C. Mei
Department of Civil Engineering
Massachusetts Institute of Technology
Cambridge, MA 02139

Professor E. Mollo-Christensen
Department of Meteorology
Room 54-1722
Massachusetts Institute of Technology
Cambridge, MA 02139

Professor J. Nicholas Newman
Department of Ocean Entineering
Room 5-324A
Massachusetts Institute of Technology
Cambridge, MA 02139

Dr. S. Orszag
Flow Research, Inc.
1 Broadway
Cambridge, MA 02142

Director
Office of Naval Research Branch Office
536 South Clark Street
Chicago, IL 60605

Library
Naval Weapons Center
China Lake, CA 93555

Professor E. Reshotko
Division of Chemical Engineering Science
Case Western Reserve University
Cleveland, OH 44106

Commander
Charleston Naval Shipyard
Naval Base
Charleston, SC 29408

Professor J. M. Burgers
Institute of Fluid Dynamics and
Applied Mathematics
University of Maryland
College Park, MD 20742

Professor Pai
Institute for Fluid Dynamics and
Applied Mathematics
University of Maryland
College Park, MD 20740

Technical Library
Naval Weapons Surface Center
Dahlgren Laboratory
Dahlgren, VA 22418

Computation & Analyses Laboratory
Naval Weapons Surface Center
Dahlgren Laboratory
Dahlgren, VA 22418

Dr. R. Chan
JAYCOR
1401 Camino Del Mar
Del Mar, CA 92014

Dr. J. A. Young
JAYCOR
1401 Camino Del Mar
Del Mar, CA 92014

Dr. R. H. Kraichnan
Dublin, NH 03444

Technical Documents Center
Building 315
Army Mobility Equipment Research Center
Fort Belvoir, VA 22060

Technical Library
Webb Institute of Naval Architecture
Glen Cove, NY 11542

Professor E. V. Lewis
Webb Institute of Naval Architecture
Glen Cove, NY 11542

Dr. M. Poreh
Technion-Israel Institute of Technology
Department of Civil Engineering
Haifa, Israel

Dr. J. P. Breslin
Davidson Laboratory
Stevens Institute of Technology
Castle Point Station
Hoboken, NJ 07030

Mr. C. H. Henry
Stevens Institute of Technology
Davidson Laboratory
Castle Point Station
Hoboken, NJ 07030

Dr. D. Savitsky
Davidson Laboratory
Stevens Institute of Technology
Castle Point Station
Hoboken, NJ 07030

Dr. A. Strumpf
Davidson Laboratory
Stevens Institute of Technology
Castle Point Station
Hoboken, NJ 07030

Professor J. F. Kennedy, Director
Institute of Hydraulic Research
University of Iowa
Iowa City, IA 52242

Professor L. Landweber
Institute of Hydraulic Research
University of Iowa
Iowa City, IA 52242

Dr. D. E. Ordway
Sage Action, Incorporated
P. O. Box 416
Ithaca, NY 14850

Dr. D. R. S. Ko
Flow Research Inc.
1819 S. Central Avenue
Kent, WA 98031

Professor V. W. Goldschmidt
School of Mechanical Engineering
Purdue University
Lafayette, IN 47907

Professor J. W. Miles
Institute of Geophysics and Planetary
Physics, A-025
University of California, San Diego
La Jolla, CA 92093

Flow Research, Inc.
Los Angeles Division
9841 Airport Blvd., Suite 1004
Los Angeles, CA 90045

Professor A. T. Ellis
Department of Applied Mathematics
and Engineering Sciences
University of California, San Diego
La Jolla, CA 92037

Director
Scripps Institute of Oceanography
University of California
La Jolla, CA 92037

Mr. Virgil Johnson, President
Hydronautics, Incorporated
7210 Pindell School Road
Laurel, MD 20810

Mr. M. P. Tulin
Hydronautics, Incorporated
7210 Pindell School Road
Laurel, MD 20810

Commander
Long Beach Naval Shipyard
Long Beach, CA 90801

Professor John Laufer
Department of Aerospace Engineering
University of Southern California
University Park
Los Angeles, CA 90007

Lorenz G. Straub Library
St. Anthony Falls Hydraulic Laboratory
University of Minnesota
Minneapolis, MN 55414

Dr. E. Silberman
St. Anthony Falls Hydraulic Laboratory
University of Minnesota
Minneapolis, MN 55414

Library
Naval Postgraduate School
Monterey, CA 93940

Professor J. Wu
College of Marine Studies
University Delaware
Newark, DE 19711

Technical Library
Naval Underwater Systems Center
Newport, RI 02840

Office of Naval Research
New York Area Office
715 Broadway - Fifth Floor
New York, NY 10003

Professor H. G. Elrod
Department of Mechanical Engineering
Columbia University
New York, NY 10027

Engineering Societies Library
345 East 47th Street
New York, NY 10017

Society of Naval Architects and
Marine Engineers
74 Trinity Place
New York, NY 10006

Technical Library
Naval Coastal System Laboratory
Panama City, FL 32401

Professor A. J. Acosta
Department of Mechanical Engineering
California Institute of Technology
Pasadena, CA 91109

Professor H. W. Liepmann
Graduate Aeronautical Laboratories
California Institute of Technology
Pasadena, CA 91109

Professor M. S. Plesset
Engineering Science Department
California Institute of Technology
Pasadena, CA 91109

Professor A. Roshko
Graduate Aeronautical Laboratories
California Institute of Technology
Pasadena, CA 91109

Professor T. Y. Wu
Engineering Science Department
California Institute of Technology
Pasadena, CA 91109

Director
Office of Naval Research Branch Office
1030 E. Green Street
Pasadena, CA 91101

Mr. R. Wade
Tetra Tech., Inc.
Marine & Environmental Engineering Div.
630 N. Rosemead Blvd.
Pasadena, CA 91107

Professor K. M. Agrawal
Virginia State College
Department of Methematics
Petersburg, VA 23803

Technical Library
Naval Ship Engineering Center
Philadelphia Division
Philadelphia, PA 19112

Technical Library
Philadelphia Naval Shipyard
Philadelphia, PA 19112

Dr. Paul Kaplan
Oceanics, Inc.
Technical Industrial Park
Plainview, NY 11803

Chief, Document Section
Redstone Scientific Information Center
Army Missile Command
Redstone Arsenal, AL 35809

Army Research Office
P. O. Box 12211
Research Triangle Park, NC 27709

Dr. H. Norman Abramson
Southwest Research Institute
8500 Culebra Road
San Antonio, TX 78228

ONR Scientific Liaison Group
American Embassy - Room A-407
APO San Francisco 96503

Technical Library
Naval Missile Center
Point Mugu, CA 93041

Commander
Portsmouth Naval Shipyard
Portsmouth, NH 03801

Commander
Norfolk Naval Shipyard
Portsmouth, VA 23709

Office of Naval Research
San Francisco Area Office
760 Market Street, Room 447
San Francisco, CA 94102

Library
Pearl Harbor Naval Shipyard
Box 400
FPO San Francisco 96610

Technical Library
Hunters Point Naval Shipyard
San Francisco, CA 94135

Dr. Steven Crow, President
Poseidon Research
11777 San Vicente Blvd., Suite 641
Los Angeles, CA 90049

Fenton Kennedy Document Library
The Johns Hopkins University
Applied Physics Laboratory
Johns Hopkins Road
Laorel, MD 20810

Librarian
Naval Surface Weapons Center
White Oak Laboratory'
Silver Spring, MD 20910

Dr. Byrne Perry
Department of Civil Engineering
Stanford University
Stanford, CA 94305

Professor Milton van Dyke
Department of Aeronautical Engineering
Stanford University
Stanford, CA 94305

Professor J. Thompson
Department of Aerophysics and Aerospace Engineering
Mississippi State University
State College, MS 39762

Professor R. DiPrima
Department of Mathematics
Rensselaer Polytechnic Institute
Troy, NY 12181

Professor J. L. Lumley
Department of Aerospace Engineering
Pennsylvania State University
University Park, PA 16802

Editor
Applied Mechanics Review
Southwest Research Institute
8500 Culebra Road
San Antonio, TX 78206

Dr. J. W. Hoyt
Code 2501
Naval Undersea Center
San Diego, CA 92132

Technical Library
Naval Undersea Center
San Diego, CA 92132

Dr. J. P. Craven
University of Hawaii
1801 University Avenue
Honolulu, HI 96822

Technical Library
Mare Island Naval Shipyard
Vallejo, CA 94592

Office of Naval Research
Code 438
800 N. Quincy Street
Arlington, VA 22217 3 copies

Office of Naval Research
Code 200
800 N. Quincy Street
Arlington, VA 22217

Office of Naval Research
Code 210
800 N. Quincy Street
Arlington, VA 22217

Office of Naval Research
Code 211
800 N. Quincy Street
Arlington, VA 22217

Office of Naval Research
Code 212
800 N. Quincy Street
Arlington, VA 22217

Office of Naval Research
Code 221
800 N. Quincy Street
Arlington, VA 22217

Office of Naval Research
Code 473
800 N. Quincy Street
Arlington, VA 22217

Office of Naval Research
Code 480
800 N. Quincy Street
Arlington, VA 22217

Office of Naval Research
Code 481
800 N. Quincy Street
Arlington, VA 22217

Office of Naval Research
Code 1021P (ONRL)
800 N. Quincy Street
Arlington, VA 22217 6 copies

Code 2627
Naval Research Laboratory 6 copies
Washington, DC 20375

Code 4000
Naval Research Laboratory
Washington, DC 20375

Code 7706
Naval Research Laboratory
Washington, DC 20375

Mr. L. Benen (Code 0322)
Naval Sea Systems Command
Washington, DC 20362

Mr. J. Schuler (Code 032)
Naval Sea Systems Command
Washington, DC 20362

Mr. W. M. Ellsworth (Code 11)
David W. Taylor Naval Ship Research
and Development Center
Bethesda, MD 20084

Dr. W. E. Cummins (Code 15)
David W. Taylor Naval Ship Research
and Development Center
Bethesda, MD 20084

Mr. G. H. Gleissner (Code 18)
David W. Taylor Naval Ship Research
and Development Center
Bethesda, MD 20084

Mr. Paul S. Granville (Code 1541)
David W. Taylor Naval Ship Research
and Development Center
Bethesda, MD 20084

Mr. J. H. McCarthy, Jr. (Code 1552)
David W. Taylor Naval Ship Research
and Development Center
Bethesda, MD 20084

Dr. Nils Salvesen (Code 1552)
David W. Taylor Naval Ship Research
and Development Center
Bethesda, MD 20084

Code 03B
Naval Sea Systems Command
Washington, DC 20362

Mr. T. Peirce (Code 03512)
Naval Sea Systems Command
Washington, DC 20362

Library (Code 09GS)
Naval Sea Systems Command
Washington, DC 20362

Code 6034
Naval Ship Engineering Center
Center Building
Prince George's Center
Hyattsville, MD 20782

Code 6101E
Naval Ship Engineering Center
Center Building
Prince George's Center
Hyattsville, MD 20782

Code 6110
Naval Ship Engineering Center
Center Building
Prince George's Center
Hyattsville, MD 20782

Code 6114
Naval Ship Engineering Center
Center Building
Prince George's Center
Hyattsville, MD 20782

Code 6136
Naval Ship Engineering Center
Center Building
Prince George's Center
Hyattsville, MD 20782

Code 6140
Naval Ship Engineering Center
Center Building
Prince Teorge's Center
Hyattsville, MD 20782

Dr. A. Powell (Code 01)
David W. Taylor Naval Ship
Research and Development Center
Bethesda, MD 20084

Code 03
Naval Air Systems Command
Washington, DC 20361

Code 03B
Naval Air Systems Command
Washington, DC 20361

Code 310
Naval Air Systems Command
Washington, DC 20361

Code 5301
Naval Air Systems Command
Washington, DC 20361

Strategic Systems Projects Office
Department of the Navy
Washington, DC 20376

Mr. Norman Nilsen (SP 2022)
Strategic Systems Projects Office
Department of the Navy
Washington, DC 20376

Oceanographer of the Navy
200 Stovall Street
Alexandria, VA 22332

Commander
Naval Oceanographic Office
Washington, DC 20373

Dr. A. L. Slafkosky
Scientific Advisor
Commandant of the Marine Corps (Code AX)
Washington, DC 20380

Librarian Station 5-2
Coast Guard Headquarters
NASSIF Building
400 Seventh Street, SW
Washington, DC 20591

Office of Research and Development
Maritime Administration
441 G Street, NW
Washington, DC 20235

Dr. W. B. Morgan (Code 154)
David W. Taylor Naval Ship Research
and Development Center
Bethesda, MD 20084

Division of Ship Design
Maritime Administration
441 G Street, NW
Washington, DC 20235

Air Force Office of Scientific
Research/NA
Building 410
Bolling AFB
Washington, DC 20332

Chief of Research and Development
Office of Chief of Staff
Department of the Army
Washington, DC 20310

Dr. G. Kulin
Fluid Mechanics Section
National Bureau of Standards
Washington, DC 20234

National Science Foundation
Engineering Division
1800 G Street, NW
Washington, DC 20550

Science and Technology Division
Library of Congress
Washington, DC 20540

Mrs. Joanna Schot (Code 1843)
David W. Taylor Naval Ship Research
and Development Center
Bethesda, MD 20084

Library (Code 5641)
David W. Taylor Naval Ship Research
and Development Center
Bethesda, MD 20084

Defense Research and Development Attache
Australian Embassy
1601 Massachusetts Avenue, NW
Washington, DC 20036